Indonesian Journal of Electrical Engineering and Computer Science
Vol. 3, No. 2, August 2016, pp. 356 ~ 368
DOI: 10.11591/ijeecs.v3.i2.pp356-368

Performance Evaluation of Fractal Array Antenna for Small Satellite Applications

Yemane Ghebremedhin Teklehaimanot, Sinshaw Bekelle, Mohammed Ismail
Tigray Regional State, Agency for Science and Technology, Ethiopia,
Mekelle, Phone: (+251) 344404132, Fax: (+251) 344418361, Tigray Region for Science and Technology
Corresponding author, e-mail: yemanri@gmail.com, ermohammedib@gmail.com

Abstract

The possible antenna which can be integrated with relatively large flat structure of solar panel of small satellites is patch antenna. The main problem of common Microstrip patch antennas is that they only operate at one or two frequencies, restricting the number of bands that equipment is capable of supporting. Another issue is that, due to the very strict space that a solar panel has, setting up more antenna array is very difficult. To reduce these problems, the use of fractal shaped antennas integrated on solar cells will be analyzed. The small satellite applications demand a high efficient multi-band antenna with a very compact size. A 2x2 Sierpinski Fractal antenna array is modeled and simulated using HFSS. The proposed work has resulted in multiband operation 10.2 GHz and 18.3GHz with increased bandwidth and radiation characteristics betterment, with added advantage of light weight and smaller dimension which is important where cost to payload is a constraint in satellites.

Keywords: *Sierpinski fractal, geometric iteration function, antenna integration in solar panel*

1. Introduction

The possible antenna which can be integrated with relatively large flat structure of solar panel of small satellites is patch antenna. The main problem of common Microstrip patch antennas is that they only operate at one or two frequencies, restricting the number of bands that equipment is capable of supporting. Another issue is that, due to the very strict space that a solar panel has, setting up more antenna array is very difficult. To reduce these problems, the use of fractal shaped antennas will be analyzed. Small satellite applications demand a high efficient multi-band antenna with a very compact size.

There are many studies done related to the integration of antennas on solar cells based on type of material used for antenna, feeding techniques of antenna, geometrical shape of antenna, different type of antenna and based on the performance of the antenna, some of them are: Vaccaro S, et al., [1] designed a linear dipole shaped slot antenna on the back side of solar cell panel and has got a high gain. But since the physical structure of small satellite is exposed to various mechanical vibrations from polar surface of the earth, make it difficult to implement for small Satellite applications. The important lesson taken from this was that antenna to be integrated on solar cell array need to be placed on the upper side and not at the back side of the solar panel. B. Sadasiva Rao, et al., [2] have designed rectangular Microstrip slot antenna on the layered antenna. Two straight parallel slots with same length and type of material are presented. But those cannot operate and perform well at higher frequencies due to the capacitive behavior they have. Timothy, et al., [3] have designed a meshed patch antenna which aimed to maximize the incident ray to the solar cell array. A meshed antenna came as an alternative to antennas made of transparent materials .But the feeding technique designed made it impractical, that is it considered to solder the feed with the fragile structure of conductive film oxides. A. Tombak, et al., [4] have designed an antenna slot on the upper side of solar panel considering the gap between the solar array cells. The effect of mechanical failure on the back side of the panel is solved but it affects the total power harvesting capacity of solar cell, where its only primary source is from the incident solar rays. S.H. Wi, et al., [5] have designed crossed slot antenna that have equal shape and size placed on a circular substrate. Promising gain was obtained, but due to the doubled thickness at the center crossed section a significant loss resulted. G. Manjo Kumar, et al., [6] have designed an elongated T shaped slot

Received March 2, 2016; Revised June 25, 2016; Accepted July 10, 2016

patch antenna, with unique concept of probe feed designed in thick microfiber reinforced substrate material having acceptable parameters. M. Tariqul Islam, et al., [7] have designed 4x1 L-probe Fed Inverted E-H Microstrip patch antenna array. This study shows a significant difference in the range of operating frequency. R. Sing, et al., [8] designed a triangular geometry antenna capable of operating in C band, which is applicable in GPS and Low Earth Orbited Satellites with acceptable antenna parameters performance. However, the proposed material is expensive to manufacture in larger scale. Asadulah Noor, et al., [9] Designed an x-shaped, circular and truncated Microstrip patch in three layered substrate with two feed points. They have achieved good circular polarization at limited beam width. However the three layered antenna has tripled substrate thickness and the X-shaped has a doubled layer at the cross points and has a direct incident light blockage effect. F Yang, et al., [10] designed E shaped Microstrip antenna with promising performance. However it requires an improvement on the Voltage standing wave ratio (VSWR) feed point location polarization. Vaccaro, et. al., [11] have developed Integrated solar cell antennas with great success, in which specifically designed solar cells are intimately combined with printed antennas, providing a new device called SOLANT. To obtain antennas and solar cells allowing a perfect and optimized combination, it is necessary to work on both domains during all of the phases of development. Xueyao Ren, et al., [12] has designed a stacked Microstrip Antenna array with fractal patches using Guiseppe peano fractal shaped patches and adopts two layer stacked structure for achieving both high gain and wideband width. However its manufacturing difficulty and the layered structure makes it difficult to implement in solar panels. Mahmoud [13], designed, a linear array antennas consisting of two series elements. The structure has two substrates, the lower substrate for the feeding network and the upper for the slot antennas etching. A layer of solar cells is integrated with antennas on the top layer. For the feed layer a Microstrip line was etched and this line is then divided using a tee junction to the two elements. This antenna may be subjected to coupling effect.

From the literatures review, we see that significant contributions have been made by many researchers for the development of antenna integration on solar cell of small satellites. However they had the design limitations of lower Bandwidth and single band operation. In this thesis geometrical shape is considered for further antenna performance improvement and reduction of size. This is very important for Satellites, because the cost to payload is a very important constraint.

2. Research Method

2.1. Design of Patch

The operating frequency of the antenna under consideration is specified and geometry is decided considering a rectangular patch t. Width and length of the rectangular patch has effect on performance of the patch antenna and to avoid cross polarization, keep 1 < W/L <1.5 [14]. First, select a recommended dielectric material of height h, having a relative Permittivity(ε_r), with specified dissipation factor $\tan\delta$.

1. To determine the width the feed (w_f), Width of patch(w): The characteristic impedance of the patch is defined in Equation (1).

$$Z_0 = \frac{120\pi}{\sqrt{\varepsilon_{reff}}\left(1.393+\frac{w_f}{h}+\frac{2}{3}\ln\left(\frac{w_f}{h}+1.444\right)\right)} \quad (1)$$

Where Z_0 = 50Ω, w_f= width of feed and h=height of the substrate, ε_{reff} effective dielectric constant.

a. Determine Width (W) of patch that leads to good radiation efficiency.

$$W = \frac{C_0}{2f_r}\sqrt{\frac{2}{\epsilon_r+1}} \quad (2)$$

Where, C_0=speed of light, f_r= Resonant frequency, ϵ_r= Dielectric constant

b. Calculate effective dielectric constant.

$$\varepsilon_{reff} = \frac{\varepsilon_r+1}{2} + \frac{\varepsilon_r-1}{2\sqrt{1+\frac{12h}{W}}} \quad (3)$$

c. Calculate effective Length.

$$\frac{\Delta L_{eff}}{h} = .412 \frac{(\varepsilon_{reff}+0.3)(\frac{W}{h}+0.264)}{(\varepsilon_{reff}-0.258)(\frac{W}{h}+0.264)(\frac{W}{h}+0.8)} \quad (4)$$

d. Calculate actual length.

$$L = \frac{Co}{2fr\sqrt{\varepsilon_{reff}}} - 2\Delta L \quad (5)$$

2. To determine the width and length of Microstrip transition feed:

a. Calculate the impedance of the patch:

$$Z_a = 90 \frac{\varepsilon_r^2}{\varepsilon_r-1} 2\left(\frac{L}{W}\right)^2 \quad (6)$$

Where, Z_a=characterstic impedance of the patch.

b. Calculate characteristic Impedance(Z_T) of the transition section:

$$Z_T = \sqrt{50 + Z_a}$$

c. Calculate width of transition line (W_T):

$$Z_T = \frac{60}{\sqrt{\varepsilon_r-1}} ln\left(\frac{8d}{W_T} + \frac{W_T}{4d}\right) \quad (7)$$

d. Calculate Length of transition line:

$$l = \frac{\lambda}{4} = \frac{\lambda_0}{4\sqrt{\varepsilon_{ref}}} \quad (8)$$

e. Calculate Width of 50Ω Microstrip transmission line:
Calculate length of the microstrip transmission line.

$$R_{in(x=0)} = \frac{Z_0}{Z_T} = \cos^2\left(\frac{\pi}{2} X_0\right) \quad (10)$$

f. Calculating the dimensions of the ground plane.

$$\lambda_{eff} = \frac{f_r}{c_o}\sqrt{\varepsilon_{reff}} \quad (11)$$

g. Length of ground plane $\geq \left(\frac{\lambda eff}{4}\right) 2 + L$ (12)

h. Width of ground plane $\geq \left(\frac{\lambda eff}{4}\right) 2 + W$ (13)

2.2. Fractal Geometry Iterated Function Systems (IFS)

Fractals are made up from the sum up of copies from itself, each copy smaller than the previous iteration .The generating fractals from a specific base geometry (A) is known as Iterated function systems (IFS). It consists of a set of affine transformations that include shearing, scaling, translating and rotating the current stage to result in the next stage of iteration [15-16]. These iterated function systems are based on the application of a series of affine transformations, *w*, defined by Equation (14).

$$W(A)=w_1(A) + w_2(A) + w_3(A) + \cdots + w_n(A). \quad (14)$$

The number of self-similar copies, the scaling ratio and the fractional area of iterated Sierpinski fractal geometry, can be calculated respectively using the three equations given below.

$$N_n = 8^n \quad (15)$$

$$L_n=(1/3)^n \quad (16)$$

$$A_n = (8/9)^n \quad (17)$$

Where, N_n is the number of copies of basic shape (Rectangle), L_n is the ratio of length and/or width, A_n is the ratio for fractional area after n^{th} iteration.

IFS works by applying a series of affine transformations w, to an elementary shape A through many iterations. The affine transformation w, for second iterated Sierpinski fractal geometry (SFG) is given by Equation (18):

$$\begin{aligned}
w_1(x,y) &= \left[\frac{1}{3}x, \frac{1}{3}y\right] \\
w_2(x,y) &= \left[\frac{1}{3}x, \frac{1}{3}y + 1/3\right] \\
w_3(x,y) &= \left[\frac{1}{3}x, \frac{1}{3}y + \frac{2}{3}\right] \\
w_4(x,y) &= \left[\frac{1}{3}x + \frac{1}{3}, \frac{1}{3}y\right] \\
w_5(x,y) &= \left[\frac{1}{3}x + \frac{1}{3}, \frac{1}{3}y + \frac{2}{3}\right] \\
w_6(x,y) &= \left[\frac{1}{3}x + \frac{2}{3}, \frac{1}{3}y\right] \\
w_7(x,y) &= \left[\frac{1}{3}x + \frac{2}{3}, \frac{1}{3}y + \frac{1}{3}\right] \\
w_8(x,y) &= \left[\frac{1}{3}x + \frac{2}{3}, \frac{1}{3}y + \frac{2}{3}\right]
\end{aligned} \quad (18)$$

Where, x is the dimension of the rectangle in the x-plane, y is the dimension of the rectangle in the x-plane and 1/3 is the scaling factor.

2.3. Design Parameters

To determine the optimal dimension of fractal patch antenna array, the first step is to find the dimensions of the patch, feed and ground. Ansoft HFSS is then used to model and tune. The single patch antenna is designed and tuned to get optimal radiation characteristics.

First iterated Sierpinski fractal is generated from the patch by applying Sierpinski fractal iteration geometry function and the antenna dimensions attained after tuning are listed in Table 1.

Table 1. Dimension of First Iterated Patch Element

Dimension	All in millimeters
Patch Width	9.9
Patch Length	8.2
Cut out Width	3.3
Cut out Length	2.73
Feed Width	0.2
Feed Length	2.6
Ground (WxL)	25mmX20mm

The first Iterated Sierpinski fractal patch antenna designed is used to realize a 2x2 fractal patch antenna array. The first iterated patch is subjected to second iteration from which 2x2 second iterated patch antenna array is realized and is shown in Figure 1. The design parameters are listed in Table 2. Second fractal geometry is generated from the first iterated patch using Sierpinski fractal geometry iteration function. Accordingly each first iterated rectangular patch which has eight similar small rectangles is divided in to nine smaller rectangles. Then all the center rectangles are dropped or cut from each rectangle to reveal second iterated Sierpinski fractal patch.

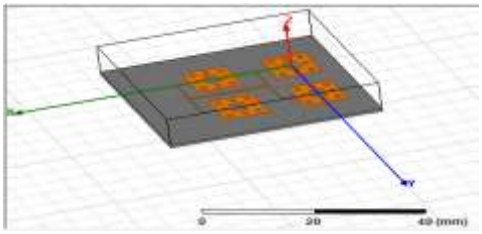

Figure 1. Second iterated SFA array HFSS model

Table 2. Dimension of second iterated SFA patch element

Dimension of Second Iterated SFA in reference to figure 13	Millimeter square
External size of rectangle (width x length)	9.9x8.2
Central big cutout rectangle (width x length)	3.3x2.73
Eight Smaller rectangles cutout each (width x length)	1.1x 0.91
Feed (width x length)	0.2x2.6

3. Results and Discussion

To evaluate the influence of fractal geometry and inter-element spacing on antenna radiation characteristics, effect of inter-element spacing in E and H planes on antenna radiation characteristics is studied for 2x2 first and second iterated fractal antenna array in the following section.

3.1. Performance Evaluation of 2x2 First Iterated SFA Array

To evaluate the influence of inter-element space variation in E plane and H plane on antenna radiation characteristics, the performance of the designed first iterated SFA array is evaluated for inter-element spacing starting from 0.5λ and going up to 0.7 λ in steps of 0.05 λ. The parameters chosen for evaluating the performance are discussed in the following sections:

3.1.1. Resonance Frequency

The inter element spacing in E and H-plane is varied from 0.5 to 0.7λ in steps of 0.05 λ and its influence on the operating frequencies of the fractal antenna is studied. This is shown in Figure 1. And the results tabulated in Table 3.

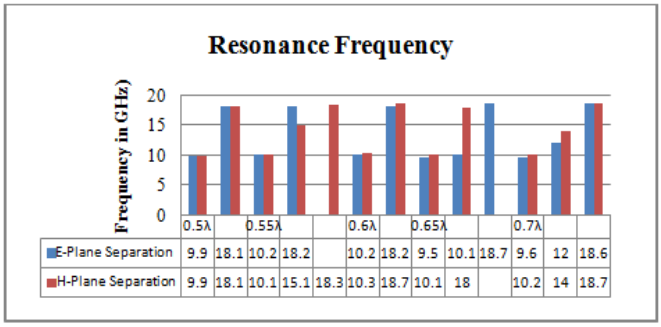

Figure 2. Inter- element spacing versus resonant frequency

From Table 3, we can infer that for overall value of inter-element spacing, both in E and H- plane, the fractal antenna operates dual or multiple frequencies and for inter-element spacing of 0.5 λ both in E and H- plane, the fractal antenna operates from 10GHz to18.1GHz.

3.1.2. Return Loss

The inter-element spacing is varied in steps of 0.05 λ varied from 0.5 λ and upto0.7 λ and its effect on the return loss of fractal antenna is studied.

Table 3. Resonant frequency for Figure 2

E-Plane Spacing	Resonant Frequency (GHz)	H-Plane Spacing	Resonant Frequency (GHz)
0.5λ	9.90	0.5λ	9.90
	18.10		18.10
0.55λ	10.20	0.55λ	10.1
	18.20		15.1
			18.3
0.6λ	10.2	0.6λ	10.3
	18.2		18.7
0.65λ	9.5	0.65λ	10.1
	10.1		18.0
	18.7		
0.7λ	9.6	0.7λ	10.2
	12.0		14.0
	18.6		18.7

This is shown in Figure 3 and the return loss tabulated in Table 4.

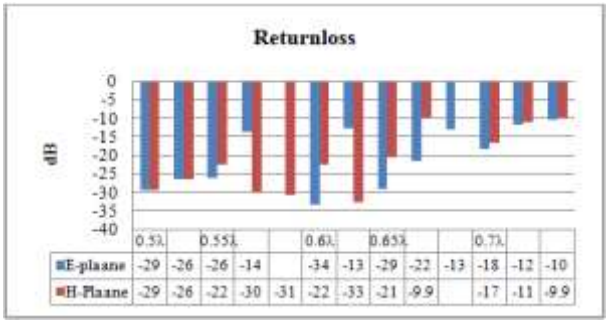

Figure 3. Effect of inter-element spacing in E and H plane on return loss

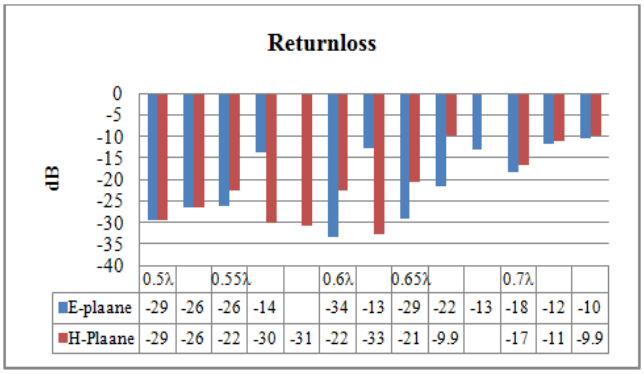

Table 4. Return loss for Figure 2

E-Plane Separation	S_{11}(dB)	H-Plane separation	S_{11}(dB)
0.5λ	-29.3890	0.5λ	-29.3890
	-26.4103		-26.4103
0.55λ	-26.1553	0.55λ	-22.4703
			-30.1452
			-30.9041
0.6λ	-33.5522	0.6λ	-22.4474
	-12.8447		-32.8239
0.65λ	-29.1098	0.65λ	-20.7354
	-21.7170		-9.8548
	-13.1311		
0.7λ	-18.2921	0.7λ	-16.7527
	-11.9406		-11.2590
	-10.4337		-9.9253

From Table 4, we see that the radiation loss in almost all the distance of separation is less than-10dB which is in the desired value.

3.1.3. Radiated Power

The amount of radiated power is found to be different for different inter-element spacing in E- and H-plane this is shown in Figure 4 and the value are tabulated in Table 5.

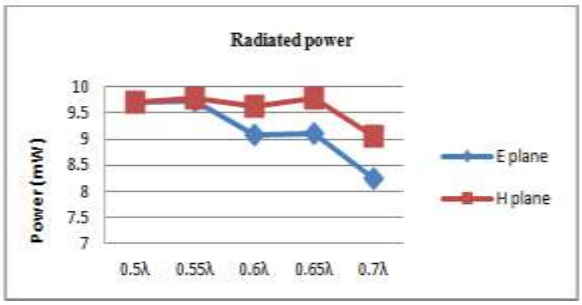

Figure 4. Effect of inter element spacing in E and H-plane versus radiated power

From Table 5 we can infer that the power radiated is at maximum of 9.785mw for 0.55 λ H palne separation. However for 0.5 λ in E and H planes there are no side lobes, radiated power is 9.712mw.

3.1.4. Directivity

The enter-element spacing is varied in steps of 0.05 from 0.5 λ to 0.7 λ and its effect on antenna directivity is studied. This is shown in Figure 5 and results tabulated in Table 6.

Table 5. Radiated power for Figure 4

E-Plane Separation	Power Radiated (mW)
0.5λ	9.7121
0.55λ	9.7331
0.6λ	9.0712
0.65λ	9.1084
0.7λ	8.2553
H-Plane Separation	**Power Radiated (mW)**
0.5λ	9.7121
0.55λ	9.785
0.6λ	9.6302
0.65λ	9.7936
0.7λ	9.049

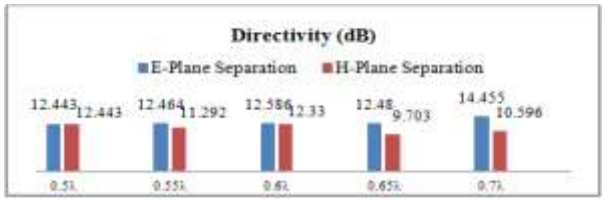

Figure 5. Peak Directivity

Table 6. Peak Directivity for Figure 4

E-Plane Separation	Peak Directivity (dB)
0.5λ	12.443
0.55λ	12.464
0.6λ	12.586
0.65λ	12.480
0.7λ	14.455
H-Plane Separation	**Peak Directivity (dB)**
0.5λ	12.443
0.55λ	11.292
0.6λ	12.33
0.65λ	9.703
0.7λ	10.596

From Table 6 we infer that the maximum peak directivity at 14.45dB for H-plane separation of 0.7 λ.

3.1.5. Gain

The effect of enter-element spacing in E and H-plane on antenna gain is studied. This is shown in Figure 6 and the results tabulated in Table 7.

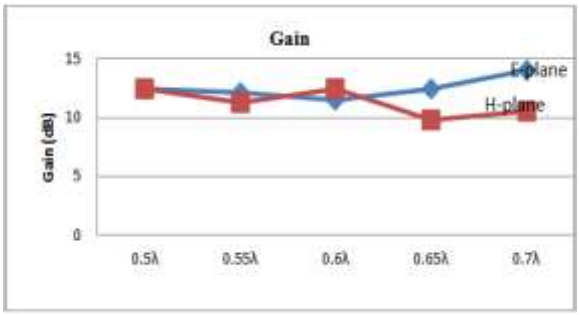

Figure 6. Effect of inter-element spacing in E plane and H plane versus peak antenna gain

Table 7. Antenna peak gain for Figure 6

E-Plane Separation	Peak Gain (dB)
0.5λ	12.438
0.55λ	12.131
0.6λ	11.499
0.65λ	12..434
0.7λ	14.053
H-Plane Separation	**Peak Gain (dB)**
0.5λ	12.438
0.55λ	11.230
0.6λ	12.309
0.65λ	9.701
0.7λ	10.508

From Table 7, we get the best gain of 14.05 for E- plane separation of 0.7 λ.

3.1.6. Antenna Input Impedance.

The ideal value of antenna impedance is expected to be 50 ohms ,so that it matches the impedance of the line. To study the influence of inter-element spacing in E and H-plane has on radiation pattern. Study is made and plotted in Figure 7, with the results tabulated in Table 8. From Table 8, we see that the antenna impedance is near to 50ohms with a value of 49.06 for E plane separation of 0.5 λ where the corresponding operating frequency is 18.10GHz.

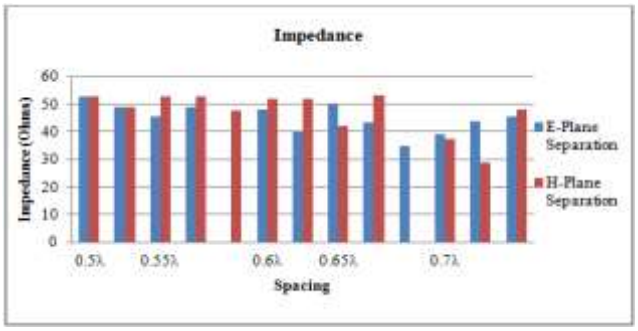

Figure 7. Effect of inter-element spacing in E and H- plane versus antenna impedance

Table 8. Antenna impedance for Figure 7

E-Plane Separation	Impedance (Ohms)	H-Plane Separation	Impedance (Ohms)
0.5λ	52.7523	0.5λ	52.7523
	49.0647		49.0647
0.55λ	45.5976	0.55λ	52.6767
	49.0421		52.6021
	0		47.6230
0.6λ	48.0288	0.6λ	51.6798
	39.8206		52.0328
0.65□	49.9196	0.65□	41.8726
	43.1973		53.2540
	34.7825		0
0.7□	39.1481	0.7□	37.4976
	43.7437		28.7281
	45.5323		48.0890

3.1.7. Antenna VSWR

The ideally a VSWR value of less than 2 is desirable. To study the influence of inter-element spacing on VSWR, a study is made and the result is shown in Figure 8, with result tabulated in Table 9.

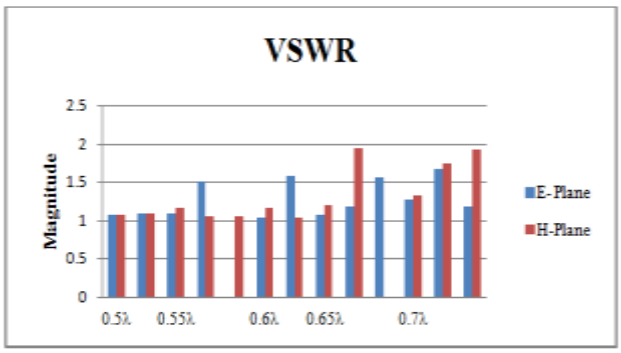

Figure 8. Effect of inter-element spacing in E and H-plane on VSWR

Table 9. VSWR for Figure 8

E-Plane Separation	VSWR	H-Plane Separation	VSWR
0.5□	1.0702	0.5□	1.0702
	1.1004		1.1004
0.55□	1.0967	0.55□	1.1627
	1.5061		1.0642
	-		1.0587
0.6□	1.0429	0.6□	1.1632
	1.5904		1.0468
0.65□	1.0726	0.65□	1.2024
	1.1788		1.9479
	1.5658		-
0.7□	1.2772	0.7□	1.3401
	1.6771		1.7531
	1.1779		1.9367

From Table 9, we can infer that the VSWR values at the corresponding operating frequency of about 10GHz in all cases is close to one.

3.1.8. Bandwidth

To study the influence of inter-element spacing in E and H-plane has on Bandwidth . Study is made and plotted in Figure 9, with the results tabulated in Table 10.

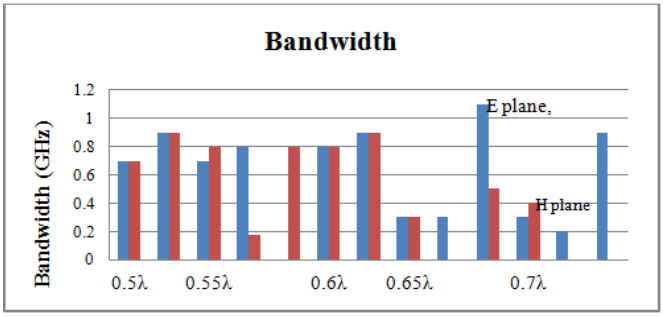

Figure 9. Effect of inter-element spacing in E and H- plane on antenna bandwidth

From Table 10, we can see that the highest bandwidth is at 0.65λ in E plane 1100MHz. Generally there is significant amount of bandwidth that this fractal antenna array can cover.

3.2. Performance Evaluation of 2x2 second Iterated SFA Array

In the previous section we see that the first iterated 2x2 fractal antenna array exhibits excellent BW and radiation characteristics for E and H plane separation of 0.5λ. This is ideal because at 0.5 λ inter-element spacing, the radiation characteristics will not have any side lobes. Hence the second iterated fractal antenna array is evaluated for 0.5 λ inter-element spacing against the following antenna parameters:

Table 10. Bandwidth for Figure 9

Element Spacing	E plane Bandwidth (MHZ)
	700
0.5λ	900
	700
0.55λ	800
	800
0.6λ	900
	300
	300
0.65λ	1100
	300
	200
0.7λ	900
Element Spacing	**H plane Bandwidth (MHZ)**
	700
0.5λ	900
	800
	176.2
0.55λ	800
	800
0.6λ	900
	300
	-
0.65λ	500
	400
	-
0.7λ	-

3.2.1. Returnloss

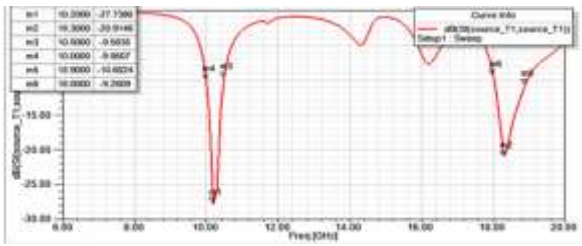

Figure 10. Return loss at 0.5λ E plane & H-plane separation between elements

3.2.2. Antenna Impedance

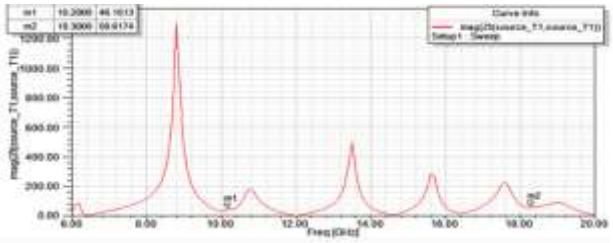

Figure 11. Impedance at 0.5λ E plane & H-plane separation between elements

3.2.3. VSWR

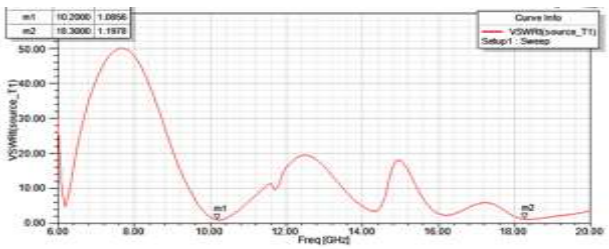

Figure 12. VSWR at 0.5λ E plane & H-plane separation between elements

The HFSS simulation of the second iterated fractal array is tabulated in Table 12.

Table 12. Performance evaluation of Second iterated SFA array

Antenna parameters	Simulation Results
Resonant Frequency (GHz)	10.20
	18.30
Return loss (decibels)	-27.738
	-20.915
Bandwidth (MHz)	500
	900
Impedance (Ohms)	46.1513
	58.6174
VSWR	1.0856
	1.1978
Power Radiated (milli watts)	9.0264
Peak Directivity (decibels)	12.594
Peak Gain (decibels)	12.571

From Figure 13, it is noted that the second iterated SFA array has less than -10dB return loss at two bands which signifies that the amount of power that is lost to the load and does not return as a reflection. The VSWR result shows values 1.08-1.19 which manifest that the impedance has matched to the transmission line. As listed in table 11, the peak Gain and peak directivity of the second iterated SFA array is 12.57 and 12.59 respectively with a power radiation of 9.07mw and wide to ultra wide range bandwidth.

3.3. Performance Comparison of First and Second Iterated SFA Array

Performance evaluation of the 2x2 first iterated fractal array, 2x2 Second iterated fractal array at both 0.5λ E plane & H-plane inter-element separation is listed in Table13.

Table 13. Performance of first iterated and second iterated SFA array at inter- element spacing of $\mathbf{0.5\lambda}$ in both E and H plane

References	First Iterated FSA array	Second Iterated FSA array
Minimum Frequency	9.90	10.20
	18.10	18.30
Return loss (dB)	-29.39	-27.74
	-26.41	-20.91
Band width (MHz)	700	500
	900	900
VSWR	1.07	1.08
	1.10	1.19
Power Radiated (mW)	9.71	9.03
Patch element area ($mm^{2)}$	72.16	64.14
Peak Gain (dB)	12.438	12.57
Directivity (dB)	12.443	12.59

From Table 13, we can infer that the second iterated SFA operates over 10.2 and 18.3 GHz, bandwidth is considerably good with appreciable amount of gain, directivity and radiated power. Also the patch element area is reduced from 72.16 mm^2 to 64.12mm^2, an effective reduction of 8.02 mm^2 that will contribute to reduced load which is a critical requirement when cost to payload is a constraint.

4. Conclusion

The proposed study revealed that there is a tremendous improvement in bandwidth with the second iterated SFA array operating at 10.3GHz and 18.30GHz which lie within the range over which the Satellites operate.

Also for 0.5 λ inter- element spacing in E and H plane of the First iterated SFA array, the proposed fractal patch antenna array integrated on solar cells of small satellites exhibits multiband operation from about 9.9GHz to 18.1GHz for S_{11} < -0 dB. The bandwidth is about

700MHz and 900MHz at each resonance frequency for S_{11} < -10 dB. The second iterated SFA array also exhibits excellent radiation characteristics but with an advantage of about 21% reduction in an element area compared to a conventional patch element. Also the fractal patch antenna array will contribute to lower weight and smaller dimension which will save the cost per payload.

Acknowledgements

The authors would like to acknowledge Tigray Regional Agency for Science and Technology, Ethiopia, for supporting this study.

References

[1] Vacacaro S, et al. In-Flight Experiment for Combined Planar Antennas and Solar Cells (SOLANT). *IET Microwave Antenna Propagation.* 2009; 3.
[2] B Sadasiva Rao, et al. Dimensional characterization of Rectangular Microstrip slots Antenna. *International Journal of Scientific advanced Research and Technology.* 2012; 2.
[3] Timothy W Truipin. Meshed patch feasibility study and optimization. Thesis. Logan, UT: Department of Electrical and computer Engineering, USU; 2008.
[4] A Tombak, et al. *An X band Low cost Compact Phased Array Based on The Extended Resonance Power Dividing Technique*. IEEE APS International Conference on Antennas Propagation. Washington DC. 2009; 3.
[5] SH Wi, et al. *Bow tie shaped Meander slot Antenna.* IEEE International Symposium Antenna and Propagation. 2002.
[6] G Manjo Kumar, et al. Design and Analysis of Narrow Inserted T shaped and Fan-wing Shaped slot patch Antenna. *International Journal of Advanced Scientific Research and Technology*. 2012.
[7] M Tariqul, et al. A 4x1 L-probe fed Inverted Hybrid E-H Microstrip patch antenna Array. *American Journal of Applied Sciences.* 2007.
[8] R Singh, et.al. Comments on An Improved Formula for Resonant Frequency of Triangular Microstrip patch Antenna. *IEEE Antenna and Propagation Society.*2001; 34.
[9] Asadulah Noor. Design of Microstrip Patch Antennas. Master Thesis. Jonkoping, Sweeden; 2012.
[10] F Yang, et al. Wide-band E- shaped Patch Antenna for Wireless Communications. *IEEE Transactions on Antennas and propagations.* 2001.
[11] Vaccaro S, et al. Integrated Solar Panel Antennas. 2000.
[12] Xueyao Ren, et al. *International Journal of Antennas and Propagation*. 2014.
[13] Mahmoud, Mahmoud N, Baktur Rahyan, Burt Robert. *Fully Integrated Solar Panel Slot Antenna for Small Satellites.* 24th Annual AIAA/USU Conference on Small Satellite. 2012.
[14] Constantine A Balanis. Antenna Theory Analysis and Design. Third Edition. John Wiley and Sons Inc. 2005.
[15] Wojeciech J Krzysztofik. Fractal Geometry in Electromagnetic application from Antenna to Metamaterial. *Microwave review.* 2013.
[16] Sierpinski Carpet Fractal Antenna for Multiband Applications. *International Journal of Computer Applications*. 2012; 39(14).